Available online at www.sciencedirect.com

ScienceDirect

Energy Procedia 159 (2019) 292–297

Energy Procedia

www.elsevier.com/locate/procedia

Applied Energy Symposium and Forum, Renewable Energy Integration with Mini/Microgrids, REM 2018, 29–30 September 2018, Rhodes, Greece

Ramp rate abatement for wind energy integration in microgrids

G. F. Frate[a], P. Cherubini[a], C. Tacconelli[b], A. Micangeli[b], L. Ferrari[a,*], U. Desideri[a]

[a] *Department of Energy, Systems, Territory and Constructions Engineering, University of Pisa, Largo Lucio Lazzarino, Pisa 56122, Italy*
[b] *Department of Mechanical and Aerospace, Sapienza University of Rome, Via Eudossiana 18, Rome 00184, Rome*

Abstract

This study analyses the performance of a battery storage system in abating the ramp rates of the power produced by a wind turbine. This approach can reduce the wind power fluctuations that are typical of small size wind farms and promote the wind energy integration in microgrids. Production data was generated from actual wind measurements over one year, and the capability of ramp abatement by varying battery capacity, battery power rating and ramp rate thresholds was investigated. The effect on battery degradation due to charge-discharge cycling required by the smoothing service was also estimated. Results suggest that good smoothing performance can be achieved with a wide range of power-capacity combinations, but the lifetime of the storage system can be as low as one year if its capacity is small.

Keywords: wind energy; ramp rate abatment; battery storage; liftime estimation

1. Introduction

Wind power is a continuously growing renewable energy source, reaching a technological maturity that makes it competitive on the market and viable without subsidies[1]. Integration of wind farm production into power grids poses many challenges due to the intermittent and fast-changing nature of the resource. Wind turbine production is typically characterized by strong ramp rates which may require production curtailment to prevent congestion or high investment in ancillary services [2]. Energy storage systems can help to reduce these negative impacts, but the economic impacts

* Corresponding author. Tel.: +39 050 221 7132; fax: +39 050 221 7333.
E-mail address: lorenzo.ferrari@unipi.it

10.1016/j.egypro.2019.01.013

are not negligible [3, 4]. Battery energy storage systems in particular have recently been investigated for their capability to provide decoupled voltage and frequency control even in a standalone network [5]. In [6] is shown how the demand response capability of electric vehicles to maintain the output wind power ramp rates between prescribed limits. Wind energy fluctuations can be particularly critical in microgrids or isolated users. Uriarte et al. [7] have investigated the effect of renewable sources ramp rates on the stability of microgrids that can be islanded from the main grid. On the other hand, wind power has a great potential to provide access to energy to remote communities that do not have access to the grid. The potential for sub-kilowatt wind turbines has been discussed in [8] and 0.8 million off-grid households are already estimated to have reached energy access through small wind turbines[9]. Wind could also provide a huge opportunity to power community-scale microgrids or hybridize those that already exist but are powered by diesel generators [10,11]. Similar efforts have already been made in countries with huge resource potential such as Kenya, as reported in [12], where the integration of the renewable resources has not been seamless, and the majority of the demand is still served by diesel generators. Therefore, there is a need coming from various applications to make wind generation more dispatchable and more easily interconnectable with a power grid or with other energy sources in isolated system. Wind generation ramp rates end up causing voltage and frequency issues in grids or supply limitations in microgrids, which can effectively be limited using energy storage [13]. The first contribution of this paper, is to analyze the wind generation ramp smoothing in a realistic scenario, using actual wind production data to test the smoothing performance of a range of battery systems with various storage and power ratings. The second contribution is the investigation of the effect of different ramp rates thresholds and how their value affects the battery durability.

2. Case Study

2.1. Obtaining the actual power output of the turbine from the wind data

The wind data used for the study comes from a wind farm in Costa Rica [14] with anemometers situated at a 50 m above the ground. The data series consisted in wind speed data averaged over 10 minutes, coupled with the standard deviation over that time span. The granularity of the data was subsequently increased to a 1-minute interval by generating 10 points randomly extracted from a gaussian distribution having the mean and the standard deviation obtained by the anemometers every 10 minutes. This a simplified, but conservative, approach as it does not take into account the autocorrelation typical of wind speed series. A more detailed analysis would be out of the scope of the study whose main purpose is to investigate the smoothing effect of energy storage on wind generation. In addition, by considering a Gaussian distribution, the “virtual” data points are more fluctuating in comparison to those generated by a distribution which respects the auto-correlation. This wind speed data was used to generate a correspondent set of generated power, by using a piece-wise fit based on the power curve of a commercial wind turbine with a rated power of 200 kW (Hummer H25.0-200KW) [15], which was considered as suitable for the case study. These power values should be considered as ideal, as they do not take into account the inertia of the turbine. Tang et al. [16] have shown that the actual turbine time constant τ is related to its natural time constant τ_0 as reported in Eq. 1:

$$\tau = \tau_0 \cdot \frac{v_{rated}}{v} \tag{1}$$

The rated speed is a characteristic given by the manufacturer. In general terms, τ_0 is the time constant of the turbine when reaching its rated rotational speed under its rated torque from a stop condition. To estimate the τ_0 of the turbine based on its rated power, a two-term power function to fit the data presented in [16] was used. This dataset was used to adjust the ideal power output as obtained from the power curve by using,

$$P_t = P_{t-\Delta t} + (P_t^{id} - P_{t-\Delta t}) \cdot (1 - e^{-\Delta t/\tau}) \tag{2}$$

where Δt is equal to the chosen sampling time, 60s. The final output of these processes is reported as histograms for wind speed and actual output power in Fig. 1.

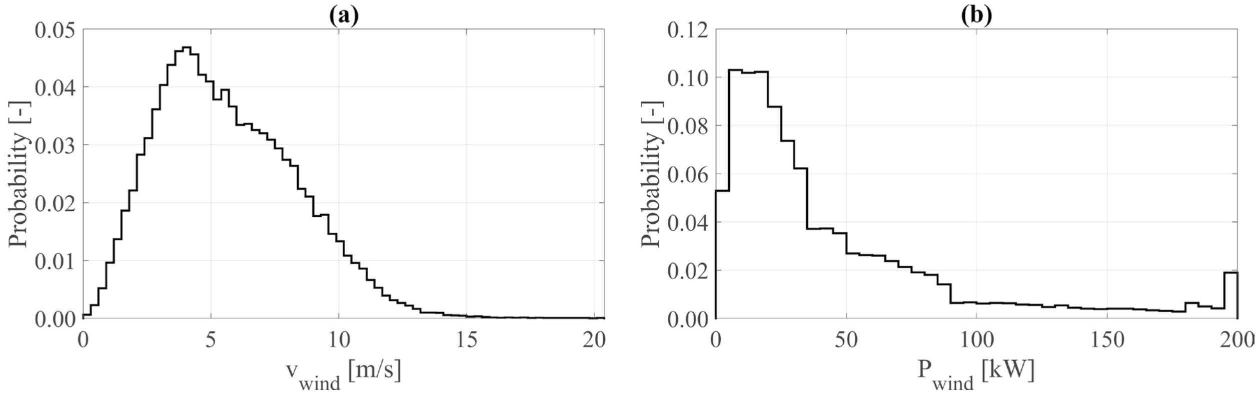

Fig. 1. (a) Histogram of the wind data series. (b) Histogram of the actual output power obtained from the turbine power curve and accounting for the turbine inertia

3. Power smoothing algorithm

The calculations have been made by accounting for three different maximum ramp rates, defined as the difference between the powers generated at two consecutive time steps, calculated as a percentage of the turbine power rating. The thresholds are set at 5%, 7.5%, 10%. A variation limit within the 10% of the rated power capacity per minute is reported in the Nordic Grid Code [17] and by the Puerto Rico Electric Power Authority[18], for example. However, the application of more stringent conditions, as could be needed in isolated system, was simulated as well. Lithium-Ion batteries were considered as a storage with a roundtrip efficiency of $\eta_{rt} = 0.9$, charge and discharge efficiencies assumed to be constant and both equal to $\eta_c = \eta_d = 0.9^{1/2}$. State of Charge (SoC) was always bound to be between 0.2 and 0.95 to prevent a quick battery degradation. Several combinations of battery capacities and power output have been considered. As a reference value for sizing the battery, the average hourly energy production was obtained from the power output of the turbine ($\bar{E}_h$) and ten values of C_b were tested, ranging from 0.1 $\bar{E}_h$ to $0.5 \cdot \bar{E}_h$. Similarly, for the battery power output, the rated power of the turbine was taken as a reference and ten values of P_b ranging from $0.1 \cdot P_{rated}$ to $0.5 \cdot P_{rated}$ were considered. The model takes into input the actual power output from the turbine and the maximum ramp size; in case the ramp exceeds the set threshold, a battery charging or discharging is necessary according to the sign of the violation. In case of a positive violation (battery charging) one has to consider the energy to be charged, the power of the battery and current SoC. Therefore, the battery is charged by considering the minimum among:

- The amount of energy to be charged into the battery to limit the ramp to the prescribed value;
- The energy that can be charged in a minute using the full power of the battery;
- The available storage capacity given by the difference between the current SoC and the maximum one.

The same logic is applied in case of a negative violation by considering the discharge capabilities of the battery. The overall procedure is outlined in Fig. 2.

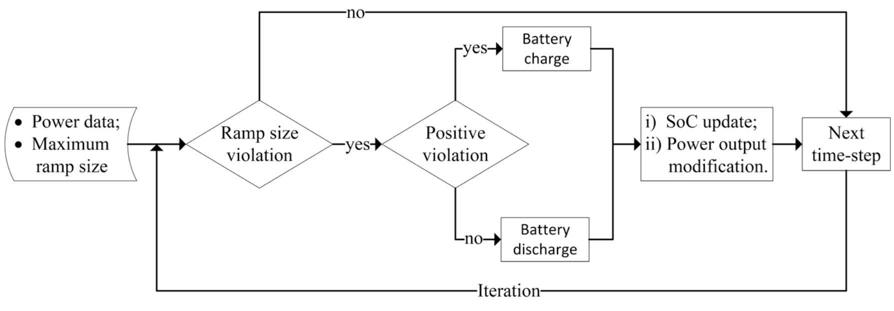

Fig. 2. Schematics of the power smoothing algorithm

In case a ramp size violation occurs, after the battery intervention, the new *SoC* and the modified output power are calculated and their value updated. This repeats for every time step. In case of a positive violation, the *SoC* has to be updated, depending on one of the three scenarios outlined above, with the following equation,

$$SoC_t = SoC_{t-\Delta t} + \min\left[\left(P_t^0 - P_{t-\Delta t} - \rho_{\max}\cdot P_{rated}\right)\cdot\Delta t, P_b\cdot\Delta t, \left(SoC_{\max} - SoC_{t-\Delta t}\right)\cdot\frac{C_b}{\eta_{rt}^{1/2}}\right]\cdot\frac{\eta_{rt}^{1/2}}{C_b} \tag{3}$$

where P^0 is the power output the turbine would have without the battery intervention and P the power output after the ramp violation correction, ρ_{max} is the maximum allowed ramp rate with respect to P_{rated} (ρ_{max} = 0.05, 0.075, 0.1). The output power in case of a positive violation is calculated with,

$$P_t = P_{t-\Delta t} - \min\left[\left(P_t^0 - P_{t-\Delta t} - \rho_{\max}\cdot P_{rated}\right)\cdot\Delta t, P_b\cdot\Delta t, \left(SoC_{\max} - SoC_{t-\Delta t}\right)\cdot\frac{C_b}{\eta_{rt}^{1/2}}\right]\Big/\Delta t \tag{4}$$

Analogously, the same must been done in case of a negative violation for the *SoC* and the output power,

$$SoC_t = SoC_{t-\Delta t} - \min\left[\left(P_{t-\Delta t} - P_t^0 - \rho_{\max}\cdot P_{rated}\right)\cdot\Delta t, P_b\cdot\Delta t, \left(SoC_{t-\Delta t} - SoC_{\min}\right)\cdot C_b\eta_{rt}^{1/2}\right]\cdot\frac{1}{C_b\eta_{rt}^{1/2}} \tag{5}$$

$$P_t = P_t^0 + \min\left[\left(P_{t-\Delta t} - P_t^0 - \rho_{\max}\cdot P_{rated}\right)\cdot\Delta t, P_b\cdot\Delta t, \left(SoC_{t-\Delta t} - SoC_{\min}\right)\cdot C_b\eta_{rt}^{1/2}\right]\Big/\Delta t \tag{6}$$

As a final output of the model, a series of smoothed power production profiles obtained for different combinations of capacity and power ratings of the batteries was obtained. These profiles have been compared with the non-smoothed profile of wind generation, to obtain a ramp abatement ratio, defined as,

$$abatement\ ratio = 1 - \frac{ramp\ violations\ in\ the\ smoothed\ profile}{ramp\ violations\ without\ the\ battery} \tag{7}$$

The results have been reported in Fig. 3 in terms of abatement ratio for different capacity and power of the batteries. In particular, $\gamma_b = C_b/\bar{E}_h$ (ratio of battery capacity over the average hourly production of the wind turbine) and $\pi_b = P_b/P_{rated}$ (ratio of the battery power over the rated power of the turbine) have been used. This allows for a better comparison of the relative values of the energy capacity and power ratings of the wind turbine and the tested battery system, while giving an idea of the energy content associated with the fluctuations of wind power output exceeding the prescribed ramp thresholds. Furthermore, the battery size expressed as (theorical) run-time hours at maximum discharge power are reported. These lines indicate batteries having the same ratio of capacity (kWh) over power (kW).

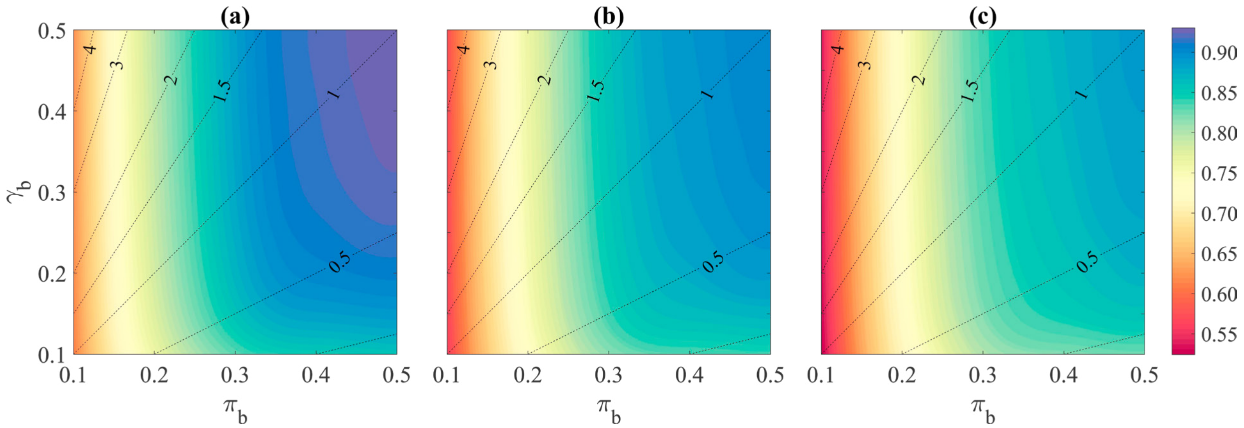

Fig. 3. Contour lines plot of the abatement ratio provided by the batteries, plotted against their nondimensionalized power ($\pi_b = P_b/P_{rated}$) and capacity ($\gamma_b=C_b/\bar{E}_h$). The dashed lines indicate the run-time hours at maximum discharge power. (a) 5% max ramp ratio (b) 7.5 % (c) 10%.

A high abatement rate of 85% can be obtained with battery power and capacity ranging from $P_b = 0.3\cdot P_{rated}$ and $C_b=0.1\cdot\bar{E}_h$, for the 5% case, to $P_b = 0.4\cdot P_{rated}$ and $C_b=0.2\cdot\bar{E}_h$ for the 10% case. However, for this system it is not possible to abate all the fluctuations: only with a maximum ramp rate of 5% batteries that have half of the power rating of the wind turbine and about half of its average hourly generation capacity are able to abate more than 90% of the ramp violations. Whereas, if the allowed ramps are larger the associated energy flows are bigger, and in the investigated range no combination of power and capacity can reach the same goal.

4. Battery degradation

The lifetime of a battery can be expressed as a number of full charge-discharge cycles it can sustain. However, the batteries performing such power-smoothing service actually undergo through an irregular pattern of micro charge-discharge cycles. The Rainflow Counting Algorithm is a technique commonly applied to estimate the battery life [19] by considering a finite number of cycle depth intervals (δ_m, which is scaled with respect to the allowable Depth of Discharge of the battery, thus comprised between 0 and 1) and counting the number of cycles in each of discharge range. The relative annual battery degradation, D_b, can be obtained by summing up the effect of all the M cycle depth intervals, through [20]:

$$D_b = \sum_{m=1}^{M} N_m \Big/ \left(A \cdot \delta_m^B \right) \tag{8}$$

Eq. 9 requires two empirical parameters, A and B, which are to be determined for each specific battery. However, a number of values for A and B are reported in the literature [19–22], and the values A=1000 and B=-1/5 have been chosen. Similarly to Fig. 3, Fig. 4 reports the results in term of battery lifetime L_b, which is the multiplicative inverse of the relative annual degradation (i.e. $L_b = 1/D_b$) as a function of π_b and γ_b.

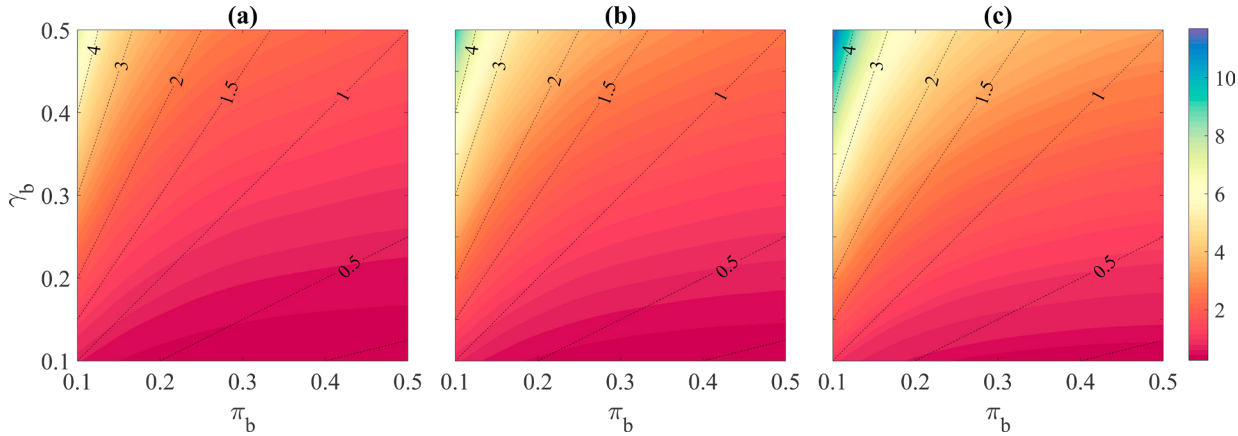

Fig. 4. Life-time in years of the batteries, plotted against their nondimensionalized power and capacity. (a) 5% max ramp ratio (b) 7.5 % (c) 10%.

By comparing Fig. 3 and Fig. 4, it can be seen that the iso-abatement curves are "more vertical" meaning that the smoothing capability depends more on the power of the batteries, whereas their durability increases more with their capacity, being the iso-lifetime curves "more horizontal". Thus, the minimum power-capacity pairings capable of guaranteeing an 85% abatement rate lead to a short lifetime, of about one year. In case (c), a 4 year durability can be reached at $C_b=0.5 \cdot \bar{E}_h$, which paired with a power $P_b = 0.4 \cdot P_{rated}$ enables an 85% ramp abatement ratio. The battery installations lasting longer than 6 years lead to an abatement ratio that can reach 70 to 75% for the three cases.

5. Conclusions

This study shows the capability of a Li-Ion battery systems in effectively abating the ramp rates of wind power production systems. Actual wind data from a windfarm in Costa Rica coupled with a 200kW wind turbine was used as a reference. A wide range of batteries capacities and powers and three values for the ramp rate threshold have been investigated. High abatement rate can be obtained with a wide range of battery power and capacity. On the other hand, the limited lifespan of battery systems showing good ramp abatement performances suggests that a thorough economic analysis has to be conducted, comparing the benefit coming from the smoothing effect with the investment cost necessary to achieve it. Furthermore, the usage of hybrid energy storage systems, comprising flywheels or ultra-capacitors, shall be looked upon as they can help decouple the power and energy requirements of the storage systems and reduce the cycling stress on the batteries.

References

[1] GWEC. Global Wind Report. Annual Market Update 2017. Glob Wind Energy Counc 2017:72.

[2] Teleke S, Baran ME, Huang a Q, Bhattacharya S, Anderson L. Control Strategies for Battery Energy Storage for Wind Farm Dispatching. IEEE Trans Energy Convers 2009;24:725–32. doi:10.1109/tec.2009.2016000.

[3] Frate GF, Peña P, Ferrari L, Desideri U. Techno-economic sizing of a battery energy storage coupled to a wind farm : an Italian case study. 73rd Conf Ital Therm Mach Eng Assoc (ATI 2018), 12–14 Sept 2018, Pisa, Italy 2018.

[4] Frate GF, Peña Carro P, Ferrari L, Desideri U. On the suitability of a battery energy storage use in a wind farm. Proc Ecos 2018 - 31st Int Conf Effic Cost, Optim Simul Environ Impact Energy Syst 2018.

[5] Hemmati R, Azizi N, Shafie-khah M, Catalão JPS. Decentralized frequency-voltage control and stability enhancement of standalone wind turbine-load-battery. Int J Electr Power Energy Syst 2018;102:1–10. doi:10.1016/j.ijepes.2018.04.021.

[6] Raoofat M, Saad M, Lefebvre S, Asber D, Mehrjedri H, Lenoir L. Wind power smoothing using demand response of electric vehicles. Int J Electr Power Energy Syst 2018;99:164–74. doi:10.1016/j.ijepes.2017.12.017.

[7] Uriarte FM, Smith C, Vanbroekhoven S, Hebner RE. Microgrid Ramp Rates and the Inertial Stability Margin. IEEE Trans Power Syst 2015;30:3209–16. doi:10.1109/TPWRS.2014.2387700.

[8] Louie H, Van Acker V, Szablya S, Dauenhauer P. Opportunities and challenges for micro wind turbines in developing communities. Proc - 2012 IEEE Glob Humanit Technol Conf GHTC 2012 2012:304–9. doi:10.1109/GHTC.2012.47.

[9] International Renewable Energy Agency (IRENA). Off-Grid Renewable Energy Systems: Status and Methodological Issues. 2015.

[10] Bianchini A, Magnelli N, Ferrara G, Carnevale EA, Ferrari L. Optimization of a PV-wind-diesel hybrid system for a remote stand-alone application. Energy Procedia 2015;81:133–45. doi:10.1016/j.egypro.2015.12.068.

[11] Ferrari L, Bianchini A, Galli G, Ferrara G, Carnevale EA. Influence of actual component characteristics on the optimal energy mix of a photovoltaic-wind-diesel hybrid system for a remote off-grid application. J Clean Prod 2018;178:206–19. doi:10.1016/j.jclepro.2018.01.032.

[12] Micangeli A, Del Citto R, Kiva I, Santori S, Gambino V, Kiplagat J, et al. Energy Production Analysis and Optimization of Mini-Grid in Remote Areas: The Case Study of Habaswein, Kenya. Energies 2017;10:2041. doi:10.3390/en10122041.

[13] Jabir M, Illias HA, Raza S, Mokhlis H. Intermittent smoothing approaches for wind power output: A review. Energies 2017;10. doi:10.3390/en10101572.

[14] Coopesantos R.L. Parque Eólico Los Santos - Energía limpia para el desarrollo. 2011.

[15] Hummer H25.0-200KW datasheet 2017. https://en.wind-turbine-models.com/turbines/1681-hummer-h25.0-200kw (accessed July 25, 2018).

[16] Tang C, Pathmanathan M, Soong WL, Ertugrul N. Effects of inertia on dynamic performance of wind turbines. 2008 Australas Univ Power Eng Conf 2008:1–6. doi:10.1109/PES.2011.6039597.

[17] Nordel. Nordic Grid Code 2007 2007;2007:69–74.

[18] Vahan G, Booth S. Review of PREPA technical requirements for interconnecting wind and solar generation. Natl Renew Energy Lab (NREL), Tech Rep NREL/TP-5D00-57089 2013:72.

[19] He G, Chen Q, Kang C, Member S, Pinson P, Xia Q, et al. Optimal bidding strategy of battery storage in power markets considering performance based regulation and battery cycle life Optimal Bidding Strategy of Battery Storage in Power Markets Considering Performance-Based Regulation and Battery Cycle Life 2016;7:2359–67. doi:10.1109/TSG.2015.2424314.

[20] Alam MJE, Saha TK. Cycle-life degradation assessment of Battery Energy Storage Systems caused by solar PV variability. IEEE Power Energy Soc Gen Meet 2016:1–5. doi:10.1109/PESGM.2016.7741532.

[21] Wang Y, Zhou Z, Botterud A, Zhang K, Ding Q. Stochastic coordinated operation of wind and battery energy storage system considering battery degradation. J Mod Power Syst Clean Energy 2016;4:581–92. doi:10.1007/s40565-016-0238-z.

[22] Bordin C, Anuta HO, Crossland A, Gutierrez IL, Dent CJ, Vigo D. A linear programming approach for battery degradation analysis and optimization in offgrid power systems with solar energy integration. Renew Energy 2017;101:417–30. doi:10.1016/j.renene.2016.08.066.